Reactions of Co, Ni, and Cu Atoms with CS_2: Infrared Spectra and Density-Functional Calculations of SMCS, M-(η^2-CS)S, M-CS_2, and MCS_2^+ in Solid Argon

Mingfei Zhou[†] and Lester Andrews*

Department of Chemistry, University of Virginia, Charlottesville, Virginia 22901

Received: October 6, 1999; In Final Form: February 17, 2000

Laser-ablated cobalt, nickel, and copper atoms and cations were reacted with CS_2 molecules during condensation in excess argon. The carbon-bonded M−η^1-CS_2 and side-bonded M−(η^2-CS)S complexes were formed on annealing, whereas the inserted SMCS molecules were formed on photolysis. The Co−η^1-CS_2^+, Ni−η^1-CS_2^+ and Cu−SCS^+ cations were also produced by metal cation reactions with CS_2. The product absorptions are identified by isotopic substitutions, electron trapping with added CCl_4, and density functional calculations. This work provides the first vibrational spectroscopic characterization of the Co, Ni, and Cu−CS_2 neutral and cation complexes and the SMCS insertion products.

Introduction

The chemistry of transition metal atoms and ions with various ligands is significant due to their important role in catalytic and biological systems. Reactions of transition metal atoms and cations with CO_2 have been investigated both by experiment[1−10] and by theory.[11−16] Complexes of first row transition metal atoms with CO_2 have been prepared in solid CO_2,[2] and reactions of laser-ablated first row transition metal atoms with CO_2 in argon have been investigated in this laboratory.[17,18] These experiments have characterized the insertion product as well as different coordination complexes. The interaction between first row transition metal cations and CO_2 has also been studied experimentally; different structural M^+-CO_2 forms have been proposed and their binding energies determined.[4−10]

The CS_2 molecule is isovalent with CO_2, but the reaction of transition metal atoms with CS_2 is relatively unexplored. The reactivity of ground and excited V^+ states and CS_2 have been examined in the gas phase using guided ion beam mass spectrometry.[19] It is interesting to compare the transition metal chemistry of CO_2 and CS_2. In this paper, we report a study of laser-ablated Co, Ni, and Cu atom and cation reactions with CS_2 in solid argon. We will show that different coordinated MCS_2 complexes and MCS_2^+ cations are formed on annealing, whereas metal insertion reactions proceed on photolysis.

Experimental and Computational Methods

The experimental methods for pulsed-laser ablation and matrix isolation infrared investigation of new chemical species have been reported previously.[20−22] The 1064-nm fundamental of a Nd:YAG laser was focused on the rotating metal target, and the ablated metal atoms were co-deposited with CS_2 molecules in excess argon onto a 10 K CsI window at 2−4 mmol/h for 1 h using laser energy from 1 to 5 mJ/pulse. Carbon disulfide and isotopic $^{13}C^{32}S_2$ (Cambridge Isotopes), $^{12}C^{34}S_2$ (Oak Ridge National Laboratory), and various mixtures were used in different experiments. A statistical sample, $^{12}C^{32}S_2$ + $^{12}C^{32}S^{34}S$ + $^{12}C^{34}S_2$, was prepared by Telsa coil discharge of a $^{12}C^{32}S_2$ + $^{12}C^{34}S_2$/Ar mixture in a quartz tube during deposition. Infrared spectra were recorded on a Nicolet 750 spectrometer at 0.5 cm^{-1} resolution and 0.1 cm^{-1} accuracy with a 77 K HgCdTe detector. Samples were annealed and subjected to photolysis using a medium-pressure mercury arc lamp and optical filters.

Density functional theory calculations were performed on metal−CS_2 species using the Gaussian 94 program.[23] The B3LYP and BP86 functionals,[24,25] the 6-311+G* basis set for C and S atoms, and the Wachters and Hay sets as modified by Gaussian 94 for cobalt, nickel, and copper atoms were employed.[26,27] Geometries were fully optimized and the vibrational frequencies computed using analytical second derivatives.

TABLE 1: Infrared Absorptions (cm^{-1}) from Co-deposition of Laser-Ablated Cobalt with CS_2 in Argon

$^{12}C^{32}S_2$	$^{13}C^{32}S_2$	$^{12}C^{34}S_2$	$R(12/13)^a$	$R(32/34)^b$	assignment
1405.3	1360.1	1398.6	1.0332	1.0048	$CoCS_2^+$
1373.0	1328.6	1366.8	1.0334	1.0045	
1363.8	1320.0	1357.5	1.0332	1.0046	
1338.7	1296.6	1332.0	1.0325	1.0050	SCoCS (0.0097)[c]
1250.3	1215.3	1241.5	1.0288	1.0071	$CoCS_2$
1173.3	1144.0	1163.4	1.0256	1.0085	Co−(η^2-CS)S (0.0086)[c]
975.3	974.4	975.0	1.0009	1.0003	$((O_2Co)(CS_2))$
973.2	972.5	972.9	1.0007	1.0003	$((O_2Co)(CS_2)$ site)
613.5	599.4	607.5	1.0235	1.0099	Co−(η^2-CS)S (0.0011)[c]
516.6	515.6	508.1	1.0019	1.0167	SCoCS (0.0008)[c]
485.2	475.1	480.1	1.0213	1.0106	$((O_2Co)(CS_2))$

[a] Frequency ratio $^{12}CO/^{13}CO$. [b] Frequency ratio $C^{32}S_2/C^{34}S_2$. [c] Maximum intensity after annealing, in a.u.

Results

Infrared Spectra. Infrared spectra were recorded for laser-ablated cobalt, nickel, and copper co-deposited with CS_2 in argon. Metal-dependent product absorptions are listed in Tables 1−3, and representative spectra are shown in Figures 1−3 including annealing and broadband photolysis behavior. Absorptions common to these experiments, namely, CS_2, CS_2^-, CS_2^+, and $(CS_2)_2^+$ have been reported in another paper,[28] and are not listed in the Tables. Experiments were done with $^{13}C^{32}S_2$, $^{12}C^{34}S_2$, and mixed $^{12}C^{32}S_2$ + $^{13}C^{32}S_2$, $^{12}C^{32}S_2$ + $^{12}C^{34}S_2$, and $^{12}C^{32}S_2$ + $^{12}C^{32}S^{34}S$ + $^{12}C^{34}S_2$ samples; the isotopic counterparts

* To whom correspondence should be addressed. E-mail: lsa@virginia.edu.
[†] Permanent address: Laser Chemistry Institute, Fudan University, Shanghai, P.R.China.

10.1021/jp993576n CCC: $19.00
Published on Web 04/20/2000

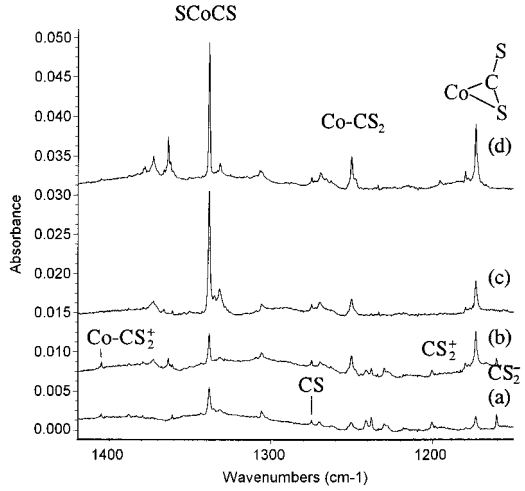

Figure 1. Infrared spectra in the 1420−1150 cm^{-1} region from co-deposition of laser-ablated Co with 0.1% CS_2 in argon: (a) after 1 h sample deposition at 10 K; (b) after annealing to 25 K; (c) after 15 min broadband photolysis; and (d) after annealing to 30 K.

TABLE 2: Infrared Absorptions (cm^{-1}) from Co-deposition of Laser-Ablated Ni with CS_2 in Argon

$^{12}C^{32}S_2$	$^{13}C^{32}S_2$	$^{12}C^{34}S_2$	$R(12/13)^a$	$R(32/34)^b$	assignment
1431.9	1386.1	1424.9	1.0330	1.0049	$NiCS_2^+$
1403.9	1358.3	1397.0	1.0336	1.0049	$((O_2Ni)(CS_2))$
1393.1	1348.0	1386.6	1.0335	1.0047	$((O_2Ni)(CS_2))$
1334.5	1293.3	1326.5	1.0319	1.0060	SNiCS
1277.4	1241.7	1268.8	1.0288	1.0068	$NiCS_2$
1208.1	1178.7	1196.6	1.0249	1.0096	Ni−(η^2-CS)S (0.031)[c]
626.0	612.1	619.5	1.0227	1.0105	Ni−(η^2-CS)S (0.0029)[c]
594.3	592.2	579.9	1.0035	1.0248	?

[a] Frequency ratio $^{12}CO/^{13}CO$. [b] Frequency ratio $C^{32}S_2/C^{34}S_2$. [c] Maximum intensity after annealing, in a.u.

TABLE 3: Infrared Absorptions (cm^{-1}) from Co-deposition of Laser-Ablated Cu with CS_2 in Argon

$^{12}C^{32}S_2$	$^{13}C^{32}S_2$	$^{12}C^{34}S_2$	$R(12/13)$	$R(32/34)$	assignment
1506.8	1458.5	1499.6	1.0331	1.0048	$CuSCS^+$
1385.5	1343.4	1377.0	1.0313	1.0062	SCuCS site
1375.5	1333.7	1367.0	1.0313	1.0062	SCuCS
1370.3	1328.3	1361.2	1.0316	1.0067	$SCuCS(CS_2)_x$
1187.4	1151.3	1180.3	1.0314	1.0060	?
1142.4	1107.6	1138.4	1.0314	1.0035	$CuCS_2$
1133.9	1101.0	1129.6	1.0299	1.0038	?
1081.9	1048.3	1076.1	1.0321	1.0054	Cu−(η^2-S_2)C
1079.7	1045.9	1073.8	1.0323	1.0055	site

are also listed in the tables, and representative spectra are shown in Figures 4−6 using a Ni target. Similar experiments were carried out with 0.02% CCl_4 added to serve as an electron trap,[18] and comparison spectra after sample deposition with Ni and Co targets are shown in Figure 7. As will be discussed, the absorptions assigned to cations were enhanced, whereas while the CS_2^- anion absorption was almost eliminated from the spectra of the deposited samples on doping with CCl_4.

Calculations. Calibration calculations for CS_2, CS_2^+ and CS_2^- are summarized in Table 4. The B3LYP calculation on CS_2 gave a 1.561/bond length, which is slightly longer than the experimental value of 1.556 Å,[29] and the antisymmetric and symmetric stretching and bending modes were predicted at 1554.6, 674.1, and 398.0 cm^{-1}, respectively, which must be multiplied by 0.987, 0.976, and 0.997 to reproduce the gas-phase experimental frequencies.[30] The BP86 calculations slightly overestimate the bond lengths and therefore produce slightly lower vibrational frequencies, which more nearly approximate the observed frequencies in most cases.

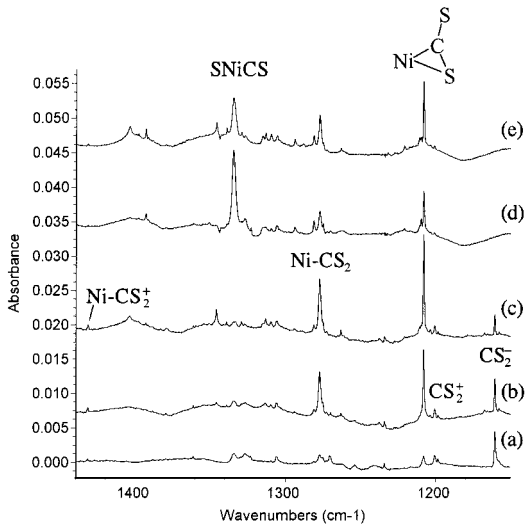

Figure 2. Infrared spectra in the 1440−1150 cm^{-1} region from co-deposition of laser-ablated Ni with 0.1% CS_2 in argon: (a) after 1 h sample deposition at 10 K; (b) after annealing to 25 K; (c) after annealing to 30 K; (d) after 15 min broadband photolysis; and (e) after annealing to 35 K.

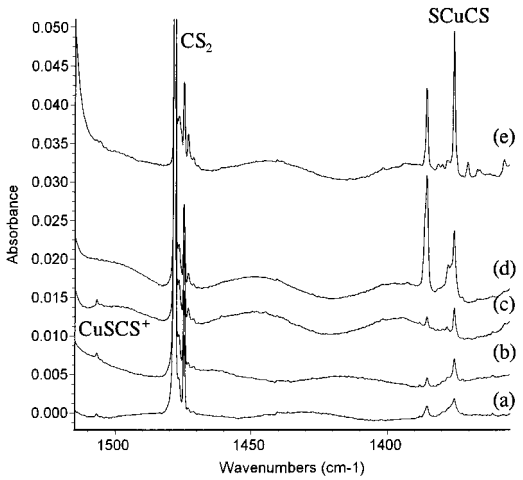

Figure 3. Infrared spectra in the 1515−1355 cm^{-1} region from co-deposition of laser-ablated Cu with 0.1% CS_2 in argon: (a) after 1 h sample deposition at 10 K; (b) after annealing to 25 K; (c) after annealing to 30 K; (d) after 15 min broadband photolysis; and (e) after annealing to 35 K.

Calculations were performed on five MCS_2 isomers and two MCS_2^+ isomers, namely, SMCS, Mn−CS_2, M−(η^2-CS)S, M−(η^2-S_2)C, symmetrical (C-bonded) M−CS_2^+ and asymmetrical (S-bonded) M−SCS^+, which are illustrated in Figure 8. The calculated geometries, relative energies, vibrational frequencies, and intensities are listed in Tables 5−10. As can be seen, the B3LYP and BP86 calculated parameters for neutral MCS_2 isomers are very similar. For Co and Ni, the M(η^2-CS)S molecule was calculated to be the most stable, followed by the symmetrical M−CS_2 and inserted SMCS molecules. For Cu, the most stable $CuCS_2$ isomer was predicted to be $^2A'$ Cu−SCS, followed by the Cu−CS_2, Cu−(η^2-S_2)C, and inserted SCuCS molecules. The Cu−(η^2-CS)S calculation converged to Cu−CS_2. However, calculations for the Co^+ and Ni^+ cations gave different results: B3LYP calculations predicted Co−SCS^+ to be 2.6 kcal/mol more stable than Co−CS_2^+, whereas the BP86 calculation on Co−SCS^+ converged to Co−CS_2^+. The B3LYP calculation found Ni−SCS^+ more stable than Ni−CS_2^+ by 3.2 kcal/mol, but the BP86 calculation predicted the Ni−CS_2^+ to

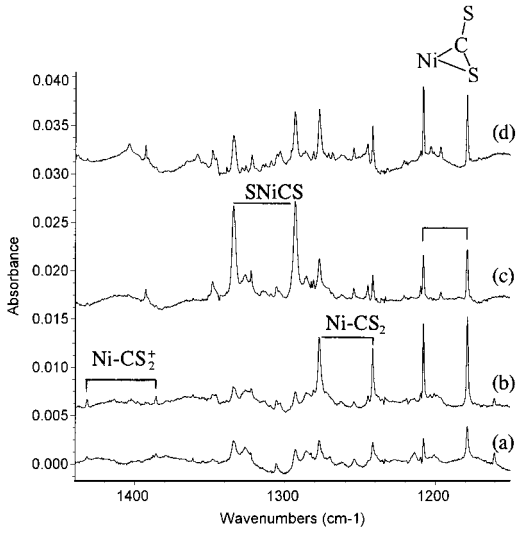

Figure 4. Infrared spectra in the 1440−1150 cm^{-1} region from co-deposition of laser-ablated Ni with 0.1% $^{12}CS_2$ + 0.1% $^{13}CS_2$ in argon: (a) after 1 h sample deposition at 10 K; (b) after annealing to 25 K; (c) after 15 min broadband photolysis; and (d) after annealing to 30 K.

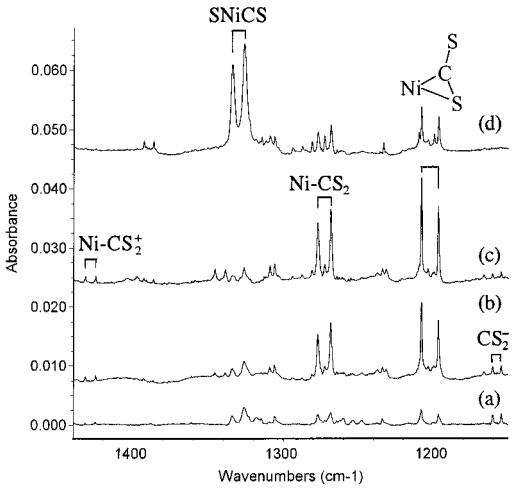

Figure 5. Infrared spectra in the 1440−1150 cm^{-1} region from co-deposition of laser-ablated Ni with 0.1% $C^{32}S_2$ + 0.1% $C^{34}S_2$ in argon: (a) after 1 h sample deposition at 10 K; (b) after annealing to 25 K; (c) after annealing to 30 K; and (d) after 15 min broadband photolysis.

be 5.4 kcal/mol more stable. Finally, both B3LYP and BP86 functionals predicted Cu−SCS^+ to be more stable than Cu−CS_2^+.

Discussion

Several new late transition metal−C,S species will be identified from spectroscopic experiment and theory.

M-(η^2-CS)S. An absorption at 1208.1 cm^{-1} in nickel experiments increased markedly on annealing but decreased greatly on broadband photolysis. It shifted to 1178.7 cm^{-1} with $^{13}C^{32}S_2$ and to 1196.6 cm^{-1} with $^{12}C^{34}S_2$, and defined the 12−32/13−32 ratio 1.0249 and the 12−32/12−34 ratio 1.0096, which suggests a C−S stretching vibration. Only pure isotopic counterparts appeared in the mixed $^{12}C^{32}S_2$+$^{13}C^{32}S_2$ and $^{12}C^{32}S_2$+$^{12}C^{34}S_2$ experiments, whereas a quartet was observed at 1208.0, 1203.5, 1200.8, and 1196.6 cm^{-1} with approximately 1:1:1:1 relative intensities in the statistically mixed $^{12}C^{32}S_2$ + $^{12}C^{32}S^{34}S$ + $^{12}C^{34}S_2$ spectra. These isotopic patterns indicate

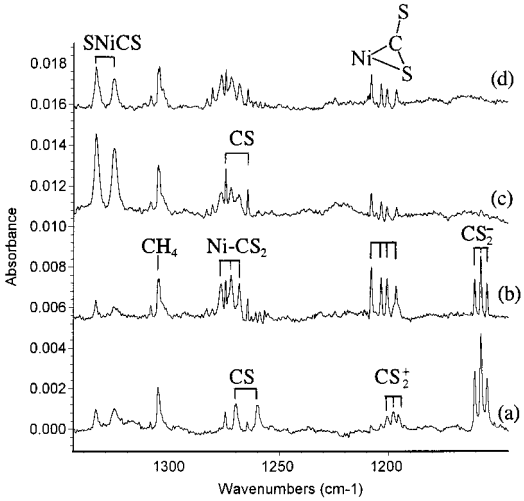

Figure 6. Infrared spectra in the 1345−1145 cm^{-1} region from co-deposition of laser-ablated Ni with 0.2% ($C^{32}S_2$ + $C^{32}S^{34}S$ + $^{34}S_2$) in argon. (a) after 1 h sample deposition at 10 K; (b) after annealing to 25 K; (c) after 15 min broadband photolysis; and (d) after annealing to 30 K.

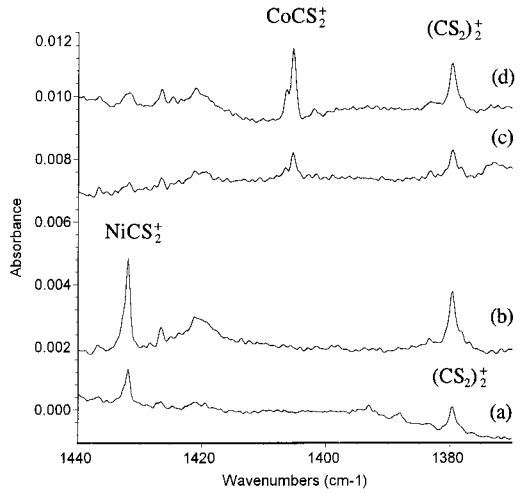

Figure 7. Infrared spectra in the 1440−1370 cm^{-1} region taken after 1 h sample deposition at 10 K in argon: (a) 0.2% CS_2/Ni; (b) 0.2% CS_2 + 0.02% CCl_4/Ni; (c) 0.2% CS_2/Co; and (d) 0.2% CS_2 + 0.02% CCl_4/Co.

that one CS_2 molecule with two *inequivalent* S atom positions is involved in this vibrational mode. The 1208.1 cm^{-1} band is assigned to the terminal C−S stretching vibration of the bridged Ni−(η^2-CS)S molecule. A weak band at 626.0 cm^{-1} showed the same annealing and photolysis behavior and similar isotopic frequency ratios and is assigned to the ring C−S stretching mode. DFT calculations predicted that the Ni−(η^2-CS)S structure ($^1A'$) is the most stable $NiCS_2$ isomer. The terminal and ring C−S stretching frequencies were calculated at 1265.0 and 631.3 cm^{-1} with B3LYP and at 1243.9 and 613.0 cm^{-1} with BP86 functionals, which are in good agreement with the observed values. The relative intensities of these two bands are predicted as 16/1 and 20/1 with the two functionals (Table 8), respectively, which is in reasonable agreement with the observed 11/1 intensity ratio.

A similar band at 1173.3 cm^{-1} in the cobalt experiments increased on annealing, decreased on photolysis, gave a statistical mixed sulfur isotopic quartet, and is assigned to the terminal C−S stretching vibration of the Co−(η^2-CS)S molecule. A weak band at 613.5 cm^{-1} tracked with the 1173.3 cm^{-1} band and is assigned to the ring C−S stretching mode of the Co−(η^2-CS)S

TABLE 4: Calculated Geometries, Vibrational Frequencies (cm^{-1}), and Intensities (km/mol) for CS_2, CS_2^+, and CS_2^-

	molecule	relative energy	geometry	frequency (intensity) (mode)	expt.[a,b,c]
B3LYP	CS_2 ($^1\Sigma_g^+$)	0	C−S:1.561Å, ∠SCS:180°	1554.6(690) (σ_u)	1533(g)
				674.1(0) (σ_g)	658
				398.0(3) (π_u)	397
	CS_2^+ ($^2\Pi_g$)	+232.6	C−S:1.560Å, ∠SCS:180°	1243.7(64) (σ_u)	1188(g)
				666.2(0) (σ_g)	617
				370.1(4) (π_u)	332
				317.3(1) (π_u)	
	CS_2^- ($^2A_1$)	−13.6	C−S:1.645Å, ∠SCS:143°	1164.1(624) (b_2))	1159(Ne)
				650.6(18) (a_1)	
				329.7(9) (a_1)	
BP86	CS_2 ($^1\Sigma_g^+$)	0	C−S:1.571Å, ∠SCS:180°	1535.7(529) (σ_u)	
				655.9(0) (σ_g)	
				382.7(4) (π_u)	
	CS_2^+ ($^2\Pi_g$)	+234.2	C−S:1.570Å, ∠SCS:180°	1292.0(42) (σ_u)	
				648.9(0) (σ_g)	
				356.7(5) (π_u)	
				306.6(1) (π_u)	
	CS_2^- ($^2A_1$)	−13.0	C−S:1.654Å, ∠SCS:143°	1145.2(539) (b_2))	
				630.1(31) (a_1)	
				322.9(13) (a_1)	

[a] Ref 30. [b] Balfour, W. J. *Can. J. Phys.* **1976**, *54*, 1969. [c] Ref 28.

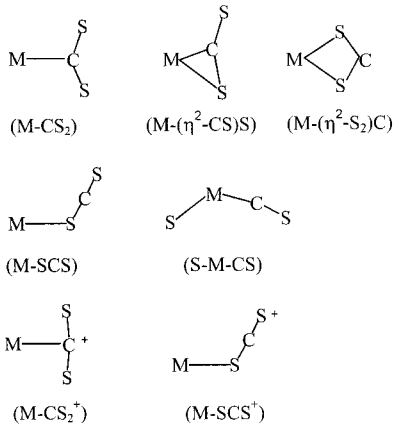

Figure 8. Geometries of different MCS_2 and M^+CS_2 isomers.

molecule. DFT calculations predicted the Co−(η^2-CS)S molecule to have a $^2A''$ ground state and to be the most stable $CoCS_2$ isomer at both BP86 and B3LYP levels of theory. The terminal and ring C−S stretching modes were calculated at 1210.2 and 629.0 cm^{-1} with B3LYP and at 1203.1 and 602.5 cm^{-1} with BP86 functionals, which adds strong support to the assignment. The relative intensities of these two bands are predicted as 22 and 33 with the two functionals (Table 6), respectively, which are higher than the observed 8/1 intensity ratio.

No obvious absorptions can be assigned to the Cu−(η^2-CS)S molecule. Our DFT calculation on doublet Cu−(η^2-CS)S converged to $^2A_1$ Cu−CS_2, suggesting that Cu−(η^2-CS)S is not a stable isomer on the potential energy surface.

MCS_2. A 1277.4 cm^{-1} band in Ni+CS_2/Ar experiments greatly increased on annealing and almost disappeared on photolysis. It shifted to 1241.7 cm^{-1} with $^{13}C^{32}S_2$ and to 1268.8 cm^{-1} with the $^{12}C^{34}S_2$ sample. In the mixed $^{12}C^{32}S_2$ + $^{13}C^{32}S_2$ and $^{12}C^{32}S_2$ + $^{12}C^{34}S_2$ experiments, only pure isotopic counterparts were produced, whereas in the mixed $^{12}C^{32}S_2$ + $^{12}C^{32}S^{34}S$ + $^{12}C^{34}S_2$ experiments, a triplet at 1277.1, 1272.6, and 1268.8 cm^{-1} with approximately 1:2:1 relative intensities was observed, indicating that one CS_2 unit with *two equivalent* S atoms is involved in this mode. This band is assigned to the antisymmetric SCS stretching vibration of the symmetrical Ni−CS_2 molecule. DFT calculation predicted a $^1A_1$ ground state for the Ni−CS_2 molecule, which is only 2.3 (B3LYP) and 3.6 kcal/mol (BP86) higher in energy than the most stable Ni−(η^2-CS)S isomer. The SCS antisymmetric stretching vibration was calculated at 1301.5 cm^{-1} with B3LYP and at 1271.7 cm^{-1} with BP86, which required 0.98(B3LYP) and 1.004(BP86) scale factors to fit the observed value, that is, the B3LYP calculation was 2% high and the BP86 functional 0.4% low.

The 1250.3 cm^{-1} band in the Co + CS_2/Ar experiments is assigned to the antisymmetric SCS stretching vibration of the Co−CS_2 molecule. This band increased on annealing and was almost eliminated on broadband photolysis. DFT calculation predicted the Co−CS_2 molecule to have a $^2A_2$ ground state, which is about 2.7 (B3LYP) and 4.1 kcal/mol (BP86) higher in energy than the most stable Co−(η^2-CS)S molecule. The antisymmetric SCS stretching vibration was calculated at 1271.3 cm^{-1} with B3LYP or at 1237.0 cm^{-1} with BP86, just 21 cm^{-1} higher or 13.3 cm^{-1} lower than the observed argon matrix value.

In the Cu + CS_2 experiments, weak bands at 1142.4 and 1081.9 cm^{-1} increased on annealing and disappeared on photolysis. The 1081.9 cm^{-1} band shifted to 1048.3 cm^{-1} with $^{13}C^{32}S_2$ and to 1076.1 cm^{-1} with $^{12}C^{34}S_2$. In the mixed $^{12}C^{32}S_2$ + $^{13}C^{32}S_2$ and $^{12}C^{32}S_2$ + $^{12}C^{34}S_2$ experiments, doublets were observed, whereas in the mixed $^{12}C^{32}S_2$ + $^{12}C^{32}S^{34}S$ + $^{12}C^{34}S_2$ experiment, a triplet with an intermediate at 1079.0 cm^{-1} was observed, indicating that one CS_2 with *equivalent S* atoms is involved in this mode. The 1142.4 cm^{-1} band shifted to 1107.6 cm^{-1} in $^{13}C^{32}S_2$ spectra and to 1138.4 cm^{-1} in the $^{12}C^{34}S_2$ spectra and also produced doublets in the mixed $^{12}C^{32}S_2$ + $^{13}C^{32}S_2$ and $^{12}C^{32}S_2$ + $^{12}C^{34}S_2$ experiments, but the mixed isotopic structure was too weak to be resolved in the mixed $^{12}C^{32}S_2$ + $^{12}C^{32}S^{34}S$ + $^{12}C^{34}S_2$ experiment. DFT calculations predicted Cu−SCS, Cu−CS_2, and Cu−(η^2-S_2)C isomers very close in energy. The CuSCS molecule was computed to have a strong C−S stretching vibration at 1493.3 cm^{-1} (B3LYP) and at 1467.4 cm^{-1} (BP86), but no band in this region can be assigned to this molecule. The Cu−CS_2 molecule was calculated to have a $^2A_1$ ground state with antisymmetric CS stretching vibrations at 1271.4 cm^{-1} (B3LYP) and at 1262.4 cm^{-1} (BP86). The Cu−(η^2-S_2)C molecule was also predicted to have a $^2A_1$ ground state with the antisymmetric CS stretching vibration at 1188.2 cm^{-1} (B3LYP) and at 1190.5 cm^{-1} (BP86). The calculated vibrational frequencies for both Cu−CS_2 and Cu−(η^2-S_2)C are higher than the observed 1142.4 and 1081.9 cm^{-1}

TABLE 5: Calculated Geometries and Relative Energies (kcal/mol) of $CoCS_2$ and $CoCS_2^+$ Isomers

	molecule	relative energy	geometry
B3LYP	Co−(η^2-CS)S′ (^{2}A″)	0	Co−C:1.810 Å, Co−S:2.176 Å, C−S:1.704 Å, C−S′:1.610 Å, ∠SCS′:149.7°
	$CoCS_2$ (^{2}A$_2$)	+2.7	Co−C:1.737 Å, C−S:1.634 Å, ∠SCS:173.2°
	SCoCS (^{2}A″)	+6.4	S−Co:2.181 Å, Co−C:1.815 Å, C−S:1.545 Å, ∠SCoC:178.9°, ∠CoCS:179.5°
	Co−(η^2-S$_2$)C (^{4}B$_1$)	+10.0	Co−S:2.298 Å, C−S:1.648 Å, ∠SCS:136.7°
	$CoCS_2$ (^{4}B$_1$)	+11.6	Co−C:1.905 Å, C−S:1.620 Å, ∠SCS:154.7°
	CoSCS (^{4}A″)	+18.3	Co−S:2.384 Å S−C:1.585 Å, C−S:1.563 Å, ∠CoSC:110.3°, ∠SCS:174.0°
	SCoCS (^{4}A″)	+20.2	S−Co:2.039 Å, Co−C:1.865 Å, C−S:1.540 Å, ∠SCoC:152.5°, ∠CoCS:162.1°
	$CoSCS^+$ (^{3}A″)	+161.6	Co−S:2.275 Å S−C:1.612 Å, C−S:1.529 Å, ∠CoSC:101.,4°, ∠SCS:174.7°
	$CoCS_2^+$ (^{3}B$_1$)	+164.2	Co−C:1.927 Å, C−S:1.591 Å, ∠SCS:176.2°
BP86	Co−(η^2-CS)S′ (^{2}A″)	0	Co−C:1.774 Å, Co−S:2.120 Å, C−S:1.735 Å, C−S′:1.617 Å, ∠SCS′:150.3°
	$CoCS_2$ (^{2}A$_2$)	+4.1	Co−C:1.722 Å, C−S:1.649 Å, ∠SCS:176.7°
	SCoCS (^{2}A″)	+4.6	S−Co:1.981 Å, Co−C:1.692 Å, C−S:1.567 Å, ∠SCoC:107.4°, ∠CoCS:174.1°
	Co−(η^2-S$_2$)C (^{4}B$_1$)	+20.2	Co−S:2.225 Å, C−S:1.673 Å, ∠SCS:131.7°
	CoSCS (^{4}A″)	+28.4	Co−S:2.282 Å, S−C:1.604 Å, C−S:1.573 Å, ∠CoSC:107.9°, ∠SCS:173.8°
	$CoCS_2^+$ (^{3}B$_1$)	+176.6	Co−C:1.840 Å, C−S:1.612 Å, ∠SCS:174.2°

TABLE 6: Calculated Vibrational Frequencies (cm^{-1}) and Intensities (km/mol) for the Structures Described in Table 5

	molecule	frequency (intensity)
B3LYP	Co−(η^2-CS)S′ (^{2}A″)	1210.2(411), 629.0(19), 502.6(2), 320.4(3), 307.0(4), 144.7(4)
	$CoCS_2$ (^{2}A$_2$)	1271.3(303), 734.2(15), 547.6(21), 240.1(0.5), 181.2(9), 43.3i(0)
	SCoCS (^{2}A″)	1360.5(631), 440.8(4), 314.1(16), 281.0(22), 271.4(28), 41.0(6)
	Co−(η^2-S$_2$)C (^{4}B$_1$)	1135.9(190), 641.6(108), 338.0(59), 279.4(0), 238.3(0.1), 227.0(1)
	$CoCS_2$ (^{4}B$_1$)	1278.6(323), 636.9(366), 510.2(23), 319.2(8), 185.3(43), 36.8(4)
	CoSCS (^{4}A″)	1494.0(614), 631.6(60), 374.3(0.5), 327.1(111), 190.2(7), 60.6(0.3)
	SCoCS (^{4}A″)	1336.6(787), 505.3(0.2), 370.5(3), 308.2(5), 276.9(30), 64.4(2)
	$CoSCS^+$ (^{3}A″)	1530.4(620), 642.9(11), 413.8(4), 365.7(5), 262.1(10), 68.1(0.4)
	$CoCS_2^+$ (^{3}B$_1$)	1419.8(360), 642.3(0.5), 529.8(5), 349.4(3), 215.9(3), 167.4(1)
BP86	Co−(η^2-CS)S′ (^{2}A″)	1203.1(329), 602.5(10), 520.5(5), 319.8(3), 312.9(5), 165.0(3)
	$CoCS_2$ (^{2}A$_2$)	1237.0(211), 776.9(8), 525.8(15), 182.3(7), 116.9(2), 73.4i(0.2)
	SCoCS (^{2}A″)	1340.0(445), 532.2(20), 468.5(4), 312.1(14), 294.4(10), 90.2(2)
	Co−(η^2-S$_2$)C (^{4}B$_1$)	1085.0(73), 623.6(82), 317.0(41), 316.1(0), 246.2(11), 196.9(0.1)
	CoSCS (^{4}A″)	1451.8(508), 606.8(23), 360.4(1), 280.1(75), 232.1(0.3), 61.8(0)
	$CoCS_2^+$ (^{3}B$_1$)	1361.3(189), 661.6(0.1), 547.0(3), 305.0(3), 224.0(4), 189.7(1)

TABLE 7: Calculated Geometries and Relative Energies (kcal/mol) of $NiCS_2$ and $NiCS_2^+$ Isomers

	molecule	relative energy	geometry
B3LYP	Ni−(η^2-CS)S′ (^{1}A′)	0	Ni−C:1.798 Å, Ni−S:2.149 Å, C−S:1.672 Å, C−S′:1.604 Å, ∠SCS′:155.4°
	$NiCS_2$ (^{1}A$_1$)	+2.3	Ni−C:1.738 Å, C−S:1.624 Å, ∠SCS:173.3°
	SNiCS (^{3}A″)	+15.3	S−Ni:2.042 Å, Ni−C:1.803 Å, C−S:1.538 Å, ∠SNiC:139.2°, ∠NiCS:169.4°
	Ni−(η^2-S$_2$)C (^{3}B$_2$)	+17.2	Ni−S:2.326 Å, C−S:1.641 Å, ∠SCS:137.5°
	Ni−(η^2-CS)S′ (^{3}A″)	+17.3	Ni−C:1.924 Å, Ni−S:2.409 Å, C−S:1.664 Å, C−S′:1.600 Å, ∠SCS′:148.7°
	$NiCS_2$ (^{3}A$_2$)	+18.1	Ni−C:1.920 Å, C−S:1.621 Å, ∠SCS:152.3°
	NiSCS (^{3}A″)	+19.3	Ni−S:2.307 Å, S−C:1.587 Å, C−S:1.563 Å, ∠NiSC:110.2°, ∠SCS:174.1°
	$NiSCS^+$ (^{2}A′)	+170.7	Ni−S:2.228 Å, S−C:1.614 Å, C−S:1.529 Å, ∠NiSC:100.4°, ∠SCS:174.2°
	$NiCS_2^+$ (^{2}B$_2$)	+173.9	Ni−C:1.988 Å, C−S:1.582 Å, ∠SCS:175.2°
BP86	Ni−(η^2-CS)S′ (^{1}A′)	0	Ni−C:1.794 Å, Ni−S:2.127 Å, C−S:1.692 Å, C−S′:1.612 Å, ∠SCS′:155.7°
	$NiCS_2$ (^{1}A$_1$)	+3.6	Ni−C:1.731 Å, C−S:1.638 Å, ∠SCS:175.2°
	SNiCS (^{3}A″)	+14.1	S−Ni:2.038 Å, Ni−C:1.767 Å, C−S:1.559 Å, ∠SNiC:135.6°, ∠NiCS:167.4°
	Ni−(η^2-S$_2$)C (^{3}B$_2$)	+29.7	Ni−S:2.242 Å, C−S:1.658 Å, ∠SCS:134.9°
	NiSCS (^{3}A″)	+37.3	Ni−S:2.233 Å, S−C:1.600 Å, C−S:1.574 Å, ∠NiSC:111.0°, ∠SCS:174.9°
	$NiCS_2^+$ (^{2}B$_2$)	+187.8	Ni−C:1.877 Å, C−S:1.602 Å, ∠SCS:174.4°
	$NiSCS^+$ (^{2}A′)	+193.2	Ni−S:2.167 Å, S−C:1.627 Å, C−S:1.543 Å, ∠NiSC:96.1°, ∠SCS:173.4°

absorptions. We tentatively assign the 1081.9 cm^{-1} band to Cu−(η^2-S$_2$)C and the 1143.4 cm^{-1} band to $CuCS_2$ based on DFT frequency calculations. Apparently, higher level calculations will be required to get better agreement.

SMCS. Sharp strong bands were observed in the 1300−1400 cm^{-1} region after broadband photolysis for all three metal systems studied here: Co, 1338.7 cm^{-1}; Ni, 1334.5 cm^{-1}; and Cu, 1375.5, 1385.5 cm^{-1}. These bands all decreased on annealing. Doublets were observed in all the mixed $^{12}C^{32}S_2 + {}^{13}C^{32}S_2$, $^{12}C^{32}S_2 + {}^{12}C^{34}S_2$, and $^{12}C^{32}S_2 + {}^{12}C^{32}S^{34}S + {}^{12}C^{34}S_2$ experiments, indicating that only one CS subunit is involved in these vibrations. The isotopic 12−32/13−32 ratios (Co, 1.0325; Ni, 1.0319; and Cu, 1.0313) are slightly higher than the diatomic CS ratio, whereas the 12−32/12−34 ratios (Co, 1.0050, Ni, 1.0060, and Cu, 1.0062) are slightly lower than the diatomic CS ratio, indicating that the C atom is vibrating between S and another atom and confirming that these vibrations are due to terminal MC−S stretching vibrations. In the case of Co, a weak absorption at 516.6 cm^{-1} tracked with the upper 1338.7 cm^{-1} band, suggesting a different mode of the same molecule. The 516.6 cm^{-1} band shifted to 515.6 cm^{-1} with $^{13}C^{32}S_2$ and to 508.1 cm^{-1} with $^{12}C^{34}S_2$, which define a small (1.0019) 12−32/13−32 ratio and a large (1.0167) 12−32/12−34 ratio and suggest that this band is due to a mostly terminal Co−S stretching vibration. Therefore, the 1338.7 and 516.6 cm^{-1} bands are assigned to the C−S and Co−S stretching vibrations of the inserted SCoCS molecule, the 1334.5 cm^{-1} band to the C−S stretching vibration of the SNiCS molecule and the 1375.5 and 1385.5 cm^{-1} bands to the C−S stretching vibration of the

TABLE 8: Calculated Vibrational Frequencies (cm^{-1}) and Intensities (km/mol) for the Structures Described in Table 7

	molecule	frequency (intensity)
B3LYP	Ni−(η^2-CS)S′ (^{1}A′)	1265.0(453), 631.3(29), 548.1(0.6), 357.5(4), 321.9(2), 136.6(3)
	$NiCS_2$ ($^1A_1$)	1301.5(352), 740.4(18), 566.7(14), 317.9(2), 192.6(5), 89.8i(0.3)
	SNiCS (^{3}A″)	1352.3(1017), 420.5(14), 356.5(23), 307.0(6), 259.3(9), 59.3(4)
	Ni−(η^2-S_2)C ($^3B_2$)	1148.2(283), 663.2(90), 363.9(34), 218.9(0), 216.9(3), 212.5(0.2)
	Ni−(η^2-CS)S′ (^{3}A″)	1247.2(401), 618.6(286), 459.8(38), 327.6(9), 229.7(13), 103.0(6)
	$NiCS_2$ ($^3A_2$)	1259.9(346), 638.5(305), 485.8(40), 321.5(8), 197.1(27), 80.0i(3)
	NiSCS (^{3}A″)	1486.7(582), 627.3(58), 370.1(0.2), 328.1(102), 212.7(1), 66.3(0.3)
	$NiSCS^+$ (^{2}A′)	1530.0(595), 642.4(9), 418.3(4), 373.1(3), 282.6(6), 73.2(0.4)
	$NiCS_2^+$ ($^2B_2$)	1471.4(414), 651.5(0.4), 492.8(2), 240.0(2), 220.1(0.6), 202.0(2)
BP86	Ni−(η^2-CS)S′ (^{1}A′)	1243.9(358), 613.0(18), 539.2(1), 339.7(5), 327.4(2), 147.0(2)
	$NiCS_2$ ($^1A_1$)	1271.7(266), 759.7(13), 546.3(11), 285.4(3), 189.1(4), 112.0i(0)
	SNiCS (^{3}A″)	1324.1(606), 481.8(4), 395.5(3), 323.6(10), 274.9(10), 64.9(2)
	Ni−(η^2-S_2)C ($^3B_2$)	1102.4(571), 649.3(83), 326.2(35), 258.5(0), 243.8(6), 96.4(0.4)
	NiSCS (^{3}A″)	1458.9(497), 609.7(23), 346.7(0.8), 316.9(57), 257.0(7), 66.6(0)
	$NiCS_2$+ ($^2B_2$)	1393.3(215), 646.8(0.1), 538.7(2), 224.3(1), 127.4(0.7), 112.1(1)
	$NiSCS^+$ (^{2}A′)	1488.4(406), 616.0(3), 395.1(5), 357.4(5), 306.5(4), 52.6(0.1)

TABLE 9: Calculated Geometries and Relative Energies (kcal/mol) of $CuCS_2$ and $CuCS_2^+$ Isomers

	molecule	relative energy	geometry
B3LYP	CuSCS (^{2}A′)	0	Cu−S:2.353 Å, S−C:1.585 Å, C−S:1.562 Å, ∠CuSC:109.8E, ∠SCS:174.0°
	$CuCS_2$ ($^2A_1$)	+2.8	Cu−C:1.974 Å, C−S:1.617 Å, ∠SCS:152.1°
	Cu−(η^2-S_2)C ($^2A_1$)	+4.4	Cu−S:2.403 Å, C−S:1.631 Å, ∠SCS:141.9°
	SCuCS ($^2\pi$)	+5.3	S−Cu:2.129 Å, Cu−C:1.825 Å, C−S:1.531 Å, linear
	$CuSCS^+$ (^{1}A′)	+152.4	Cu−S:2.238 Å, S−C:1.612 Å, C−S:1.528 Å, ∠CuSC:100.9°, ∠SCS:174.5°
	$CuCS_2^+$ ($^1A_1$)	+156.0	Cu−C:2.031 Å, C−S:1.582 Å, ∠SCS:178.8°
BP86	CuSCS (^{2}A′)	0	Cu−S:2.262 Å, S−C:1.598 Å, C−S:1.573 Å, ∠CuSC:110.4°, ∠SCS:174.2°
	$CuCS_2$ ($^2A_1$)	−0.2	Cu−C:1.925 Å, C−S:1.627 Å, ∠SCS:153.5°
	Cu−(η^2-S_2)C ($^2A_1$)	+4.5	Cu−S:2.355 Å, C−S:1.638 Å, ∠SCS:144.0°
	SCuCS ($^2\pi$)	+3.0	S−Cu:2.105 Å, Cu−C:1.803 Å, C−S:1.549 Å, linear
	$CuSCS^+$ (^{1}A′)	+157.7	Cu−S:2.185 Å, S−C:1.622 Å, C−S:1.541 Å, ∠CuSC:99.3E, ∠SCS:173.7°
	$CuCS_2^+$ ($^1A_1$)	+162.0	Cu−C:1.947 Å, C−S:1.600 Å, ∠SCS:178.8°

TABLE 10: Calculated Vibrational Frequencies (cm^{-1}) and Intensities (km/mol) for the Structures Described in Table 9

	molecule	frequency (intensity)
B3LYP	CuSCS (^{2}A′)	1493.3(571), 630.7(57), 374.7(0.3), 333.8(101), 192.9(2), 64.7(0.4)
	$CuCS_2$ ($^2A_1$)	1271.4(370), 619.5(280), 435.2(111), 348.3(11), 187.9(12), 28.0i(2)
	Cu−(η^2-S_2)C ($^2A_1$)	1188.2(331), 640.0(118), 365.5(79), 262.0(0), 170.0(0.1), 140.1(0)
	SCuCS ($^2\pi$)	1398.4(629), 431.2(2), 324.9(2), 310.5(16), 293.1(6), 63.5(1), 61.4(1)
	$CuSCS^+$(^{1}A′)	1536.9(580), 646.8(11), 423.5(4), 374.0(3), 271.7(7), 76.2(0.4)
	$CuCS_2^+$ ($^1A_1$)	1444.1(443), 645.4(0), 483.5(0.2), 374.3(4), 188.1(3), 72.2i(2)
BP86	CuSCS (^{2}A′)	1467.4(458), 614.1(28), 352.8(0.7), 317.7(70), 230.1(0.9), 67.6(0.1)
	$CuCS_2$ ($^2A_1$)	1262.4(273), 622.0(204), 472.3(38), 341.5(10), 190.2(17), 57.5i(2)
	Cu−(η^2-S_2)C ($^2A_1$)	1190.5(237), 624.0(103), 336.1(101), 247.4(0), 185.2(0.4), 58.7(0)
	SCuCS ($^2\pi$)	1356.8(522), 444.2(2), 335.6(2), 325.6(6), 290.7(7), 63.9(0.4), 57.5(1)
	$CuSCS^+$ (^{1}A′)	1502.9(427), 625.5(6), 409.2(5), 356.5(3), 296.6(4), 72.3(0.2)
	$CuCS_2^+$ ($^1A_1$)	1399.3(302), 619.9(0), 518.4(0.7), 352.4(5), 202.3(2), 65.9i(2)

SCuCS molecule at different matrix sites. The Ni−S and Cu−S stretching vibrations were not observed here.

The assignments are further supported by DFT calculations. Both BP86 and B3LYP functionals predicted the inserted SMCS molecules to be several kcal/mol higher in energy than the most stable isomers. The SCoCS molecule was calculated to have a ^{2}A″ ground state with bent geometry. The C−S and Co−S stretching frequencies were calculated at 1360.5 and 440.8 cm^{-1} with the B3LYP functional; the C−S stretching calculation fits the experiment quite well, but the S−Co stretching mode was predicted too low, as was its intensity. However, BP86 calculation predicted these two modes at 1340.0 and 532.2 cm^{-1}, in excellent agreement with the observed values. The SNiCS molecule was calculated to have a ^{3}A″ ground state with bent geometry and the C−S stretching frequency was calculated at 1352.3 cm^{-1} with B3LYP and at 1324.1 cm^{-1} with BP86. The Ni−S stretching vibration was predicted at 420.5 cm^{-1} using B3LYP and at 481.8 cm^{-1} using BP86 with much lower intensity. Both BP86 and B3LYP functional calculations found the SCuCS molecule to have a doublet ground state with linear geometry. The C−S stretching vibration was calculated at 1398.4 cm^{-1} with B3LYP and at 1356.8 cm^{-1} using BP86, which are slightly higher and lower than the observed values. The Cu−S stretching vibration was calculated at 431.2 cm^{-1} (B3LYP) and at 444.2 cm^{-1} (BP86) with much lower intensity and cannot be observed here.

The important neutral Co, Ni, and Cu atom reactions are summarized below. Reactions 1 and 2 proceed during matrix annealing without activation energy, but reaction 3 requires activation.

$$M + CS_2 \rightarrow M{-}CS_2 \ (M = Co, Ni, Cu) \quad (1)$$

$$M + CS_2 \rightarrow M{-}(\eta^2\text{-CS})S \ (M = Co, Ni) \quad (2)$$

$$MCS_2 \text{ and } M{-}(\eta^2\text{-CS})S \xrightarrow[\text{photolysis}]{\text{ultraviolet}} SMCS \ (M = Co, Ni, Cu) \quad (3)$$

MCS_2^+. Weak bands above 1400 cm^{-1} were observed for all three metal systems: Co, 1405.3 cm^{-1}; Ni, 1431.9 cm^{-1}; and Cu, 1506.8 cm^{-1}. These bands appeared on sample deposition and increased on annealing but almost disappeared

on broadband photolysis and failed to reproduce on further higher temperature annealing. As shown in Figure 7, these bands were greatly enhanced in CCl_4 doping experiments along with the $(CS_2)_2^+$ absorption,[28] which strongly suggest cation assignments as CCl_4 captures electrons and aids the survival of metal cations.[18] The 1405.3 cm^{-1} band shifted to 1360.1 cm^{-1} with the $^{13}C^{32}S_2$ sample and to 1398.6 cm^{-1} with the $^{12}C^{34}S_2$ sample and gave a 12−32/13−32 ratio 1.0332 and 12−32/12−34 ratio 1.0045. In the mixed $^{12}C^{32}S_2 + {}^{13}C^{32}S_2$ and $^{12}C^{32}S_2 + {}^{12}C^{34}S_2$ experiments, only pure isotopic counterparts were produced, indicating that only one CS_2 subunit is involved in this vibrational mode, whereas in the mixed $^{12}C^{32}S_2 + {}^{12}C^{32}S^{34}S + {}^{12}C^{34}S_2$ experiments, a weak triplet with an intermediate at 1401.9 cm^{-1} ($A = 0.0008$) was produced, suggesting that the two S atoms are equivalent in a symmetrical configuration. These observations identify $Co-CS_2^+$. Spectra were similar to the 1405.3 cm^{-1} band in Co + CS_2 experiments: the 1431.9 cm^{-1} band in Ni + CS_2 experiments shifted to 1386.1 cm^{-1} with $^{13}C^{32}S_2$ and to 1424.9 cm^{-1} with $^{12}C^{34}S_2$, doublets were produced in the mixed $^{12}C^{32}S_2 + {}^{13}C^{32}S_2$ and $^{12}C^{32}S_2 + {}^{12}C^{34}S_2$ experiments, and a weak triplet with an intermediate at 1428.5 cm^{-1} was produced in the mixed $^{12}C^{32}S_2 + {}^{12}C^{32}S^{34}S + {}^{12}C^{34}S_2$ experiment. Therefore, these bands are assigned to the symmetrical $Ni-CS_2^+$ cation. The 1506.8 cm^{-1} band in Cu + CS_2 experiments is a little different: it shifted to 1458.5 cm^{-1} with $^{13}C^{32}S_2$ and to 1499.6 cm^{-1} with $^{12}C^{34}S_2$, exhibited very similar isotopic ratios as $Co-CS_2^+$ and $Ni-CS_2^+$, and doublets were produced in the mixed $^{12}C^{32}S_2 + {}^{13}C^{32}S_2$ and $^{12}C^{32}S_2 + {}^{12}C^{34}S_2$ experiments. However, the mixed $^{12}C^{32}S_2 + {}^{12}C^{32}S^{34}S + {}^{12}C^{34}S_2$ experiment only gave a broad doublet, indicating that this band is mostly a C−S stretching vibration coupled to another *inequivalent* S atom. Hence, the 1506.8 cm^{-1} band is assigned to the $Cu-SCS^+$ cation.

DFT calculations were performed on two MCS_2^+ cation isomers, namely, $M\text{-}SCS^+$ and $M\text{-}CS_2^+$, to support the cation identifications. For Co, B3LYP calculations predicted a $^3A''$ state $Co-SCS^+$ 2.6 kcal/mol lower in energy than the $^3B_1$ state $Co-CS_2^+$, but the BP86 calculation on the $^3A''$ state $Co-SCS^+$ converged to $Co-CS_2^+$. The antisymmetric C−S stretching vibration of the $Co-CS_2^+$ cation was calculated at 1419.8 cm^{-1} (B3LYP) and at 1361.3 cm^{-1}(BP86), slightly lower than the experimental value. The C−S stretching vibration of the $Co-SCS^+$ cation was calculated at 1530.4 cm^{-1} (B3LYP), much higher than the observed value. For $Ni-CS_2^+$, the B3LYP functional predicted a $^2B_2$ ground-state $Ni-CS_2^+$, which is 3.2 kcal/mol higher in energy than the $^2A'$ state $Ni-SCS^+$. However, BP86 calculations predicted that the $^2B_2$ $Ni-CS_2^+$ form is 5.4 kcal/mol lower in energy than the $^2A''$ $Ni-SCS^+$ isomer. The antisymmetric C−S stretching vibration was calculated at 1471.4 cm^{-1} with B3LYP and at 1393.3 cm^{-1} with BP86 for $Ni-CS_2^+$. The $NiSCS^+$ isomer gave a higher C−S stretching vibrational frequency (1530.0 cm^{-1} with B3LYP and 1488.4 cm^{-1} with BP86). Apparently, the $Ni-CS_2^+$ results fit the experiment better. For Cu, both B3LYP and BP86 calculations predicted $CuSCS^+$ to be more stable than $Cu-CS_2^+$; the C−S stretching vibration of $CuSCS^+$ was calculated at 1536.9 cm^{-1} (B3LYP) and at 1467.4 cm^{-1} (BP86).

The important Co, Ni, and Cu cation reactions observed here are given below.

$$M^+ + CS_2 \rightarrow M\text{-}CS_2^+ \ (M = Co, Ni) \qquad (4)$$

$$Cu^+ + CS_2 \rightarrow CuSCS^+ \qquad (5)$$

TABLE 11: Calculated (BP86) Mulliken Charge Populations of MCS_2 Complexes and MCS_2^+ Cations

molecule	M	C	S_1	S_2
$Co-(\eta^2\text{-}CS^1)S^2$ ($^2A''$)	+0.14	+0.33	−0.19	−0.27
$Ni-(\eta^2\text{-}CS^1)S^2$ ($^1A'$)	+0.11	+0.38	−0.22	−0.27
$Co-CS_2$ ($^2A_2$)	+0.07	+0.58	−0.32	−0.32
$Ni-CS_2$ ($^1A_1$)	+0.06	+0.56	−0.31	−0.31
$Cu-CS_2$ ($^2A_1$)	+0.05	+0.48	−0.27	−0.27
$Co-CS_2^+$ ($^3B_1$)	+0.34	+0.70	−0.02	−0.02
$Ni-CS_2^+$ ($^2B_2$)	+0.31	+0.69	0.00	0.00
$Cu-CS_2^+$ ($^1A_1$)	+0.34	+0.72	−0.03	−0.03
$NiSCS^+$ ($^2A'$)	+0.47	+0.66	−0.05	−0.09
$CuSCS^+$ ($^1A'$)	+0.45	+0.71	−0.07	−0.09
CS_2 ($^1\Sigma_g^+$)		+0.60	−0.30	−0.30
CS_2^+ ($^2\Pi_g$)		+0.74	+0.13	+0.13
CS_2^- ($^2A_1$)		+0.08	−0.54	−0.54

Other Absorptions. Three weak bands at 1363.8, 975.3 and 485.2 cm^{-1} in the Co + CS_2 experiments increased together on annealing and disappeared on UV photolysis but regenerated on higher temperature annealing. The 1363.8 cm^{-1} band showed linear antisymmetric S−C−S stretching carbon and sulfur isotopic frequency ratios, indicating that this band is due to an antisymmetric S−C−S stretching mode, presumably for linear CS_2 in a complex. The 975.3 cm^{-1} band has very little C and S isotopic effect; hence, it must involve primarily other atoms. As laser-ablated Co is extremely reactive with O_2, and linear OCoO is the major product[31] (which absorbs at 945.4 cm^{-1}), the 975.3 cm^{-1} band is probably due to the antisymmetric O−Co−O stretching vibration of O−Co−O in a complex with CS_2. Neither isolated CoO nor CoO_2 was detected in these experiments, so any CoO_2 formed (probably from oxides on the cobalt target surface) is all complexed with CS_2. The 485.2 cm^{-1} band exhibited the 12−32/13−32 ratio 1.0213 and 12−32/12−34 ratio 1.0106 and is probably due to a $Co-CS_2$ vibration. Accordingly, these three bands are tentatively attributed to stretching modes of the weak $(O_2Co)(CS_2)$ complex. Similar bands at 1403.9 and 1393.1 cm^{-1} in Ni + CS_2 experiments are probably due to the same kind of complex and are tentatively assigned to the antisymmetric S−C−S stretching vibration of the $(O_2Ni)(CS_2)$ complex; the Ni−O stretching mode is probably much weaker and is not observed here. There is precedent for weak O_2 complexes with linear ORhO.[32]

Comparison with the CO_2 System. Transition metal interactions with CO_2 have been studied extensively by theory and experiment.[1−16] Earlier infrared experiments suggest that Co interacts with CO_2 to form the $Co-CO_2$ complex and with Cu to form the Cu−OCO complex.[2] Our reactions of laser-ablated Co, Ni, and Cu atoms with CO_2 produced only the inserted OMCO molecules, and failed to observe any metal−CO_2 complexes in solid argon.[18] However, under the same conditions Co, Ni, and Cu atoms react with CS_2 to form $M-CS_2$ and $M-(\eta^2\text{-}CS)S$ complexes. These complex absorptions increased on annealing, suggesting that Co, Ni, and Cu metal atoms and CS_2 reactions are exothermic and without need of activation energy. As listed in Table 11, there is a very small charge transfer from metal to CS_2, and the SCS bond angles in the $M-CS_2$ complexes are close to linear; for MCO_2 complexes, however, more charge transfer is required, with more bent OCO angles (close to CO_2^-),[11,12,18] and therefore, this reaction requires more activation energy than the corresponding CS_2 reaction.

Co^+CO_2 and Ni^+CO_2 have been studied in the gas phase, and Co^+CO_2 was found to be linear from the rotational spectrum; however, Ni^+CO_2 was proposed to have a *T*-shaped Ni^+-CO_2 structure.[8,9] However, theoretical calculations suggest that Ni^+CO_2 should also have a linear structure.[14,15] Our spectra show that both $CoCS_2^+$ and $NiCS_2^+$ have *T*-shaped C_{2v}

structures, whereas for $CuCS_2^+$, the structure is $Cu-SCS^+$. Theoretical calculations suggest that interaction between transition metal cation and CO_2 is mainly electrostatic; charge transfer and covalent interactions are smaller as the charge is mainly located on the metal center, and there is no obvious bond between the metal cation and O in the linear $M\text{-}OCO^+$ complexes.[14,15] However, as listed in Table 11, our DFT calculations suggest that there is significant charge transfer from the metal center to the CS_2 moiety in both $M-CS_2^+$ and $M-SCS^+$ isomers, which exhibit significant differences compared with MCO_2^+.

Conclusions

Laser-ablated cobalt, nickel, and copper atoms and cations were reacted with CS_2 molecules during condensation in excess argon. The $M-\eta^1\text{-}CS_2$ and side-bonded $M-(\eta^2\text{-}CS)S$ complexes are formed on annealing, whereas the inserted SMCS molecules are produced on photolysis. The MCS_2^+ cations are also produced via metal cation reactions with CS_2. The identifications of these neutral and cation product infrared absorptions are supported by density functional calculations and electron trapping with added CCl_4 to capture electrons and enhance cations. DFT calculations suggest that the $CoCS_2^+$ and $NiCS_2^+$ cations have *T*-shaped C_{2v} structures, whereas the $CuCS_2^+$ cation has a bent $Cu-SCS^+$ geometry.

Acknowledgment. We gratefully acknowledge N.S.F. support for this research under Grant No. CHE 97-00116.

References and Notes

(1) Ozin, G. A.; Huber, H.; McIntosh, D. *Inorg. Chem.* **1978**, *17*, 147.
(2) Mascetti, J.; Tranquille, M. *J. Phys. Chem.* **1988**, *92*, 2173.
(3) Galan, G.; Fouassier, M.; Tranquille, M.; Mascetti, J.; Papai, I. *J. Phys. Chem.* A **1997**, *101*, 2626.
(4) Sievers, M. R.; Armentrout, P. B. *J. Chem. Phys.* **1995**, *102*, 754.
(5) Lessen, D. E.; Asher, R. L.; Brucat, P. J. *J. Chem. Phys.* **1991**, *95*, 1414.
(6) Schwarz, J.; Schwarz, H. *Organometallics* **1994**, *13*, 1518.
(7) Schwarz, J.; Heinemann, C.; Schwarz, H. *J. Phys. Chem.* **1995**, *99*, 11405.
(8) Asher, P. L.; Bellert, D.; Buthelezi, T.; Brucat, P. *J. Chem. Phys. Lett.* **1994**, *227*, 623.
(9) Asher, P. L.; Bellert, D.; Buthelezi, T.; Weerasekera, G.; Brucat, P. *J. Chem. Phys. Lett.* **1994**, *228*, 390.
(10) Baranov, V.; Javahery, G.; Hopkinson, A. C.; Bohme, D. K. *J. Am. Chem. Soc.* **1995**, *117*, 12801.
(11) Jeung, G. *Mol. Phys.* **1989**, *67*, 747.
(12) Caballol, R.; Sanchez Marcos, E.; Barthelat, J. C. *J. Phys. Chem.* **1987**, *91*, 1328.
(13) Sodupe, M.; Branchadell, V.; Oliva, A. *J. Phys. Chem.* **1995**, *99*, 8567.
(14) Sodupe, M.; Branchadell, V.; Rosi, M.; Bauschlicher, C. W., Jr. *J. Phys. Chem. A* **1997**, *101*, 1854.
(15) Fan, H. J.; Liu, C. W. *Chem. Phys. Lett.* **1999**, *300*, 351.
(16) Papai, I.; Mascetti, J.; Fournier, R. *J. Phys. Chem. A.* **1997**, *101*, 4465.
(17) Zhou, M. F.; Andrews, L. *J. Am. Chem. Soc.* **1998**, *120*, 13230.
(18) Zhou, M. F.; Liang, B. Y.; Andrews, L. *J. Phys. Chem. A* **1999**, *103*, 2013; Zhou, M. F.; Andrews, L. *J. Phys. Chem. A* **1999**, *103*, 2066.
(19) Rue, C.; Armentrout, P. B. *J. Chem. Phys.* **1999**, *110*, 7858.
(20) Burkholder, T. R.; Andrews, L. *J. Chem. Phys.* **1991**, *95*, 8697.
(21) Hassanzadeh, P.; Andrews, L. *J. Phys. Chem.* **1992**, *96*, 9177.
(22) Zhou, M. F.; Andrews, L. *J. Chem. Phys.* **1999**, *110*, 10370.
(23) Frisch, M. J.; Trucks, G. W.; Schlegel, H. B.; Gill, P. M. W.; Johnson, B. G.; Robb, M. A.; Cheeseman, J. R.; Keith, T.; Petersson, G. A.; Montgomery, J. A.; Raghavachari, K.; Al-Laham, M. A.; Zakrzewski, V. G.; Ortiz, J. V.; Foresman, J. B.; Cioslowski, J.; Stefanov, B. B.; Nanayakkara, A.; Challacombe, M.; Peng, C. Y.; Ayala, P. Y.; Chen, W.; Wong, M. W.; Andres, J. L.; Replogle, E. S.; Gomperts, R.; Martin, R. L.; Fox, D. J.; Binkley, J. S.; Defrees, D. J.; Baker, J.; Stewart, J. P.; Head-Gordon, M.; Gonzalez, C.; Pople, J. A. GAUSSIAN 94, Revision B.1; Gaussian, Inc.: Pittsburgh, PA, 1995.
(24) Perdew, J. P. *Phys. Rev. B* **1986**, *33*, 8822. Becke, A. D. *J. Chem. Phys.* **1993**, *98*, 5648.
(25) Lee, C.; Yang, E.; Parr, R. G. *Phys. Rev. B* **1988**, *37*, 785.
(26) McLean, A. D.; Chandler, G. S. *J. Chem. Phys.* **1980**, *72*, 5639. Krishnan, R.; Binkley, J. S.; Seeger, R.; Pople, J. A. *J. Chem. Phys.* **1980**, *72*, 650.
(27) Wachters, H. J. H. *J. Chem. Phys.* **1970**, *52*, 1033. Hay, P. J. *J. Chem. Phys.* **1977**, *66*, 4377.
(28) Zhou, M. F.; Andrews, L. *J. Chem. Phys.* **2000**, *112*, 6576. (CS_2^+, CS_2^-).
(29) Suzuki, I. *Bull. Chem. Soc. Jpn.* **1975**, *48*, 1685.
(30) Wentink, T. *J. Chem. Phys.* **1958**, *29*, 188.
(31) Chertihin, G. V.; Citra, A.; Andrews, L.; Bauschlicher, C. W., Jr. *Phys. Chem. A* **1997**, *101*, 8793.
(32) Citra, A.; Andrews, L. *J. Phys. Chem. A* **1999**, *103*, 4845.